

Functionalization and Modification of Polyethylene Terephthalate Polymer by AgCl Nanoparticles under Ultrasound Irradiation as Bactericidal

Mitra Alidadykhah, Hossein Peyman,* Hamideh Roshanfekr, Shohreh Azizi,* and Malik Maaza



Cite This: *ACS Omega* 2022, 7, 19141–19151

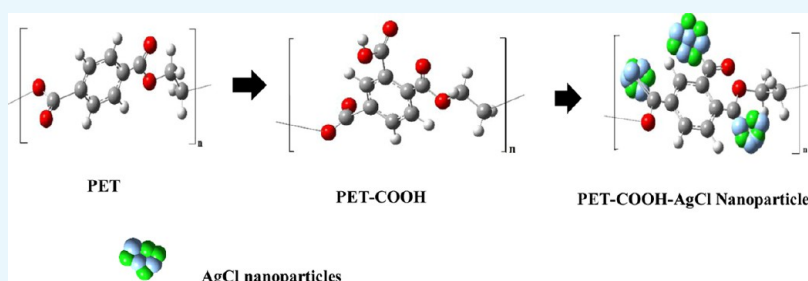


Read Online

ACCESS |

Metrics & More

Article Recommendations



ABSTRACT: Polyethylene terephthalate polymer (PET) is widely used in diverse areas. In the current study, the surface of PET is modified in two steps in order to improve the quality. At first, the polymer was functionalized with carboxylic groups, and Fourier transform infrared spectroscopy studies were used to verify functionalization. Then, AgCl nanoparticles were synthesized on COOH functional groups on the surface of PET using a sonochemistry method by sequential dipping of the functionalized polymer in an alternating bath of potassium chloride and silver nitrate under ultrasonic irradiation. The effects of ultrasonic irradiation power, the number of dipping steps, and pH on the growth of AgCl nanoparticles as effective parameters on size and density of synthesized Ag nanoparticles were studied. The results of scanning electron microscopy studies showed that the size and density of AgCl nanoparticles under ultrasonic irradiation with a power of 100 W are better than those of AgCl nanoparticles under irradiation with a power of 30 W. Also, by 15 times dipping the polymer into the reagent solutions in pH = 9, the modified polymer with a greater number of nanoparticles with suitable size can be reached. Antibacterial properties of PET containing AgCl nanoparticles were investigated against six Gram-positive and Gram-negative bacteria species, and the results showed significant antibacterial activity, while functionalized PET did not have a significant effect on both types of bacteria.

1. INTRODUCTION

Polyethylene terephthalate (PET) is a linear and aromatic polyester that is the production of reaction between terephthalic acid and ethylene glycol.^{1,2} PET composites have a wide range of industrial applications, including in packaging, construction, automotive parts, electronic equipment, and the textile industry.³ Also, this polymer is widely used in medical applications such as vascular prostheses,^{4,5} heart valve sewing cuffs,^{6,7} implantable sutures,⁸ and other surgical usage.^{9–12}

As an inert polymer with no surface reactive functional groups, modification of the PET surface can improve its hemocompatibility. Therefore, by surface functionalization, nanoparticles can be immobilized on the surface, and it subsequently could improve the desirable properties of PET.

In the recent years, hydrolysis, reduction, glycolysis, aminolysis, amination,^{9–11,13–16} and the other various techniques have been applied to introduce reactive functional groups on PET surfaces.¹⁷ Carboxylation is another technique

which introduces carboxylic groups on the PET surface without any change in bulk and surface properties. Therefore, in this study, the PET surface is modified with carboxylation in order to improve the surface properties and stabilize nanomolecules on it.

Currently, due to specific properties, nanoparticles are widely produced and used in industrial areas.¹⁸ Properties of mineral nanoparticles depend on their size and morphology. Controlled design and synthesis of nanoparticles in different size and morphology are very important in both scientific and technological fields.^{19–21} In this context, nano-crystalline silver halide coatings on some substrates with large surface areas

Received: December 15, 2021

Accepted: February 8, 2022

Published: May 31, 2022



have received major interest in recent years. Desirable optical, magnetic, catalytic, and antibacterial properties of AgCl make it a good candidate in different areas such as the photography, pharmaceutical, and electronic industry.^{22,23} Various techniques have been developed for preparing AgCl nanoparticles such as electrospinning,²⁴ template synthesis,²⁵ microemulsion,^{4,26–28} reverse micelles,²⁹ laser-based synthesis,³⁰ host-guest nanocomposite material,^{31,32} ultrasonic spray pyrolysis,³³ and sonochemistry.³⁴

In the current study, the sonochemistry method is applied to synthesize AgCl nanoparticles on the surface of functionalized PET.

Recently, the effects of ultrasonic irradiation on the chemical reactions have been reported in various studies.³⁵ In this method, molecules undergo chemical changes under powerful ultrasonic irradiation.^{36–38} All products of sonochemical reactions are in nanoscale with variety in size, shape, structure, and solid phase (amorphous or crystalline).³⁹ One of the advantages of ultrasonic irradiation is that there is no need of a surfactant and high temperature;^{40–43} also, it yields nanoparticles in smaller size.^{40,44,45} Ultrasonic irradiation accelerates chemical reactions, and those reactions that are hardly possible under normal conditions can be carried out under ultrasonic irradiation.^{46,47}

In this study, PET fibers were carboxylated and coated with AgCl nanoparticles using ultrasonic irradiation for the first time. The growth of AgCl nanoparticles on the functionalized PET fibers was reached by sequential dipping steps in an alternating bath of potassium chloride and silver nitrate.⁴⁸

2. RESULTS AND DISCUSSION

2.1. Mechanism and Characterization of –COOH Functionalization. PET functionalization was carried out in

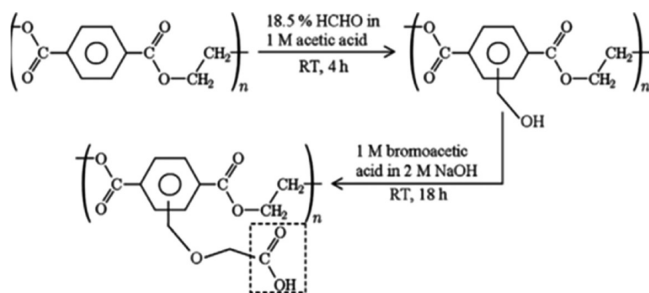


Figure 1. PET functionalized mechanism.

two steps: First, in the presence of acetic acid and formaldehyde solution, the $-\text{CH}_2\text{OH}$ group bonded to the aromatic ring. In the second step, in the presence of sodium hydroxide and bromoacetic acid solution, the $-\text{CH}_2\text{OH}$ group became deprotonated and changed into the carboxylic acid group.

The mechanism is that formaldehyde captures a proton and becomes $^+\text{CH}_2\text{OH}$ under acidic conditions. In the presence of PET, protonated formaldehyde acts as an electrophile molecule and attacks one of the double bonds in the aromatic ring via its positively charged carbon, and it leads to the formation of a transition-state intermediate. By adding NaOH, OH^- removes one of the hydrogens near formaldehyde on the aromatic ring (in the form of H_2O) leading to the formation of a stable product with the $-\text{CH}_2\text{OH}$ substituent on the aromatic ring. In an alkaline pH, the CH_2OH substituent loses

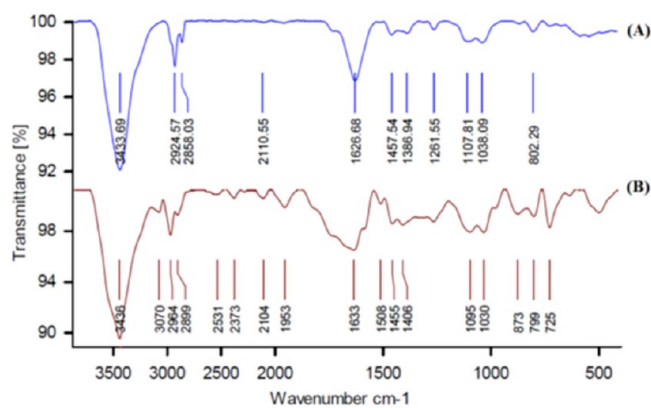


Figure 2. FT-IR spectrum of PET, (A) non-functionalized PET and (B) functionalized PET by acetic acid groups.

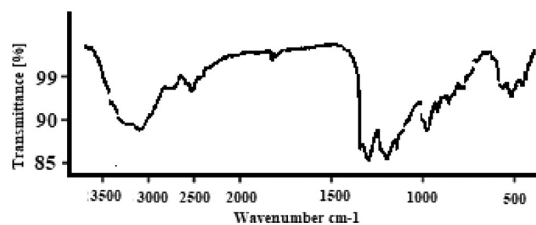


Figure 3. FT-IR spectrum of PET modified by AgCl-NPs.

its alcoholic proton in the presence of bromoacetic acid, and then, CH_2O^- attacks the carbon which is bonded to bromine in bromoacetic acid via a nucleophilic mechanism, and by removing the bromide ion, the $\text{CH}_2\text{OCH}_2\text{COO}^-$ substituent will be produced on the surface of PET (Figure 1).⁸

As shown in Figure 2, spectrum A is related to a non-functionalized PET polymer, and spectrum B is related to a functionalized PET polymer in which the $-\text{COOH}$ functional group is located on its surface.

In spectrum A, stretching vibrations of O–H at the end of the PET polymer (3433.69 cm^{-1}), esteric C=O groups (1626.68 cm^{-1}), C–O group (1038.09 and 1107.81 cm^{-1}), C=C group of aromatic rings (1457.54 cm^{-1}), CH_2-CH_2 group (2858.03 and $2924/57\text{ cm}^{-1}$), and out of plane C–H (802.29 cm^{-1}) are shown.

Generally, the stretching vibration of the esteric C=O group is located at $1735-1750\text{ cm}^{-1}$, but here, due to being near the aromatic ring, it acts as an electron-withdrawing group and conjugates with the aromatic ring that leads to reduced frequency and energy; therefore, the absorption peak of esteric C=O appears in lower frequency. The C=C group has a double stretching vibration peak (1475 and 1600 cm^{-1}), but due to being near the esteric C=O group, there is an overlapping in the spectra peak at 1600 cm^{-1} ; therefore, it appears in 1457.54 cm^{-1} .

In spectrum B, there are peaks related to the functional groups of the PET polymer and $-\text{COOH}$ functional group. Stretching vibration of O–H at the end of the polymer (3436 cm^{-1}), acidic O–H (3070 cm^{-1}), polymeric C=O (1633 cm^{-1}), and acidic C=O (1731 cm^{-1}) is shown in spectrum B. Basically, the stretching vibration frequency of acidic C=O should be lower than that of esteric C=O ($1700-1730$ and $1735-1750\text{ cm}^{-1}$, respectively), but due to the withdrawing substituent in the aromatic ring, the frequency of C=O shifted to a frequency lower than that of acidic C=O.

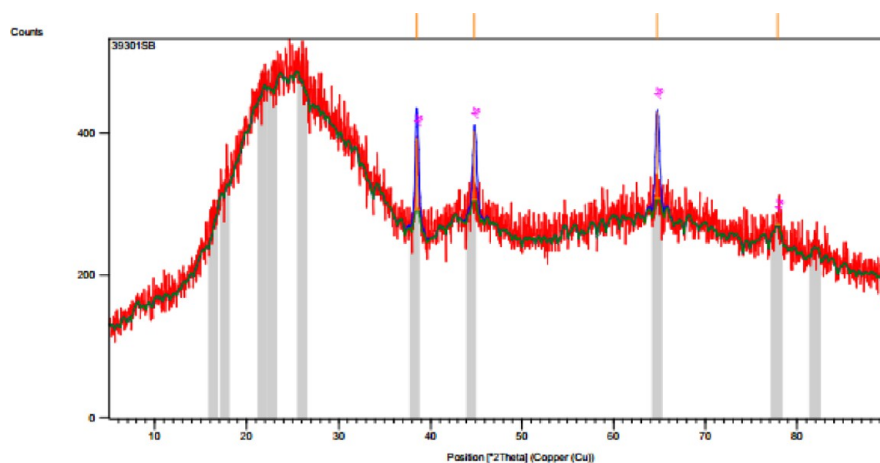


Figure 4. XRD spectrum of PET modified by AgCl-NPs.

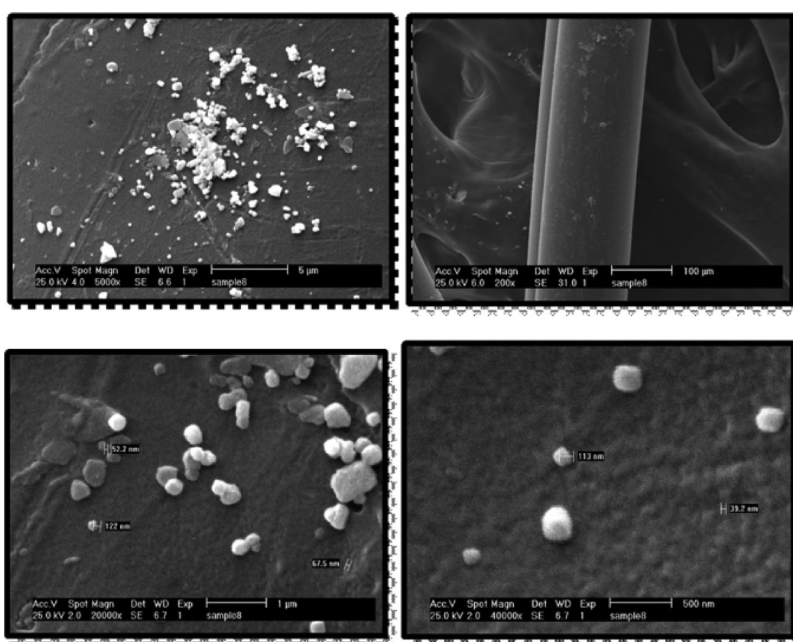


Figure 5. SEM of the blank sample (without ultrasound irradiation). 15 sequential dipping steps and pH = 9.

Stretching vibration frequencies of polymeric C–O, acidic C–O, and polymeric C=C are 1030 and 1095, 1455, and 1508 and 1582 cm^{-1} , respectively, and stretching vibration of out of plane C–H is at 799 and 873 cm^{-1} . Those stretching vibration peaks related to out of plane C–H indicate the types of substituents in the aromatic ring, and the two C=O substituents are in the para position.

2.2. Mechanism of AgCl Nanoparticle Synthesis. In alkaline pH, the surface of the polymer is negatively charged because carboxylic groups are deprotonated.^{40,48} By dipping the negatively charged polymer in AgNO_3 solution, Ag^+ ions will attach to the PET surfaces via an electrostatic bond and electron-rich atoms in the carboxylic group, and the other groups of polymers interact with the electropositive metal cations.

After the dipping step in AgNO_3 solution, rinsing the polymer will wash out those cations which are weakly attached to the other sites rather than carboxylic groups. By dipping the polymer into the KCl solution, the formation of AgCl nanoparticles is initiated. By repeating the sequential dipping

steps in the alternating bath, AgNO_3 and KCl solutions cause the growth of AgCl nanoparticles and increase their number and density.

2.2.1. Ultrasound Effects. In order to study the effect of ultrasonic irradiation on the characteristic of produced nanoparticles, the control samples were treated without ultrasonic irradiation, in which AgCl nanoparticles reached on the surfaces of the PET polymer by sequential dipping steps in the alternating bath with no ultrasonic irradiation.³⁴ The product was dried and studied by scanning electron microscopy (SEM). The results show that the average size of AgCl nanoparticles is in the range of 78.33 nm (Figure 5). The average size of AgNO_3 nanoparticles with the same sequential dipping steps and applying different ultrasonic irradiations is 65.51 and 62.33 nm for lower power (30 W) and higher power (100 W), respectively (Figures 6–7). Ultrasonic irradiation has two primary effects on a liquid: cavitation (formation, growth, and collapse of bubbles) and heating. When the bubbles collapse near the surface of a solid substrate, they make powerful, turbulent, and microjet waves that lead to the

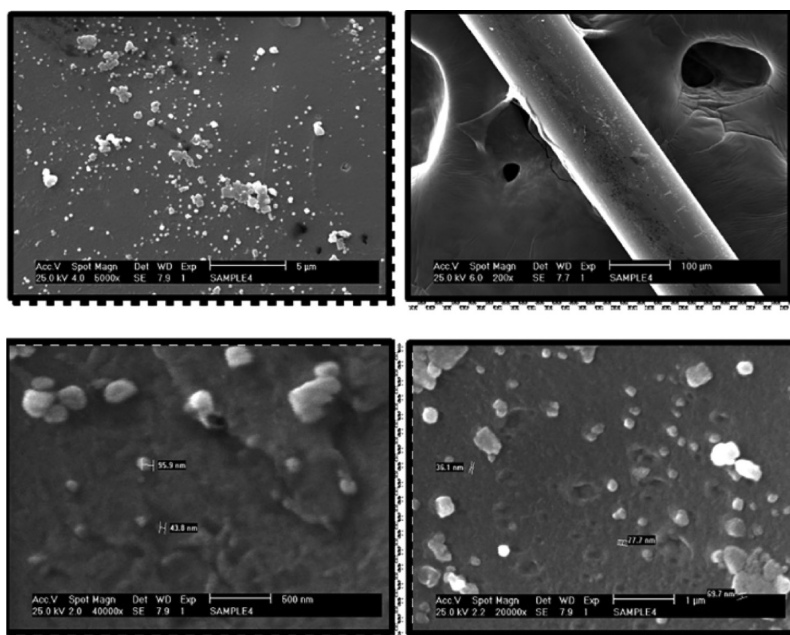


Figure 6. SEM of AgCl-NP synthesis on the PET fiber. 15 sequential dipping steps, ultrasound irradiation power 30 W, and pH = 9.

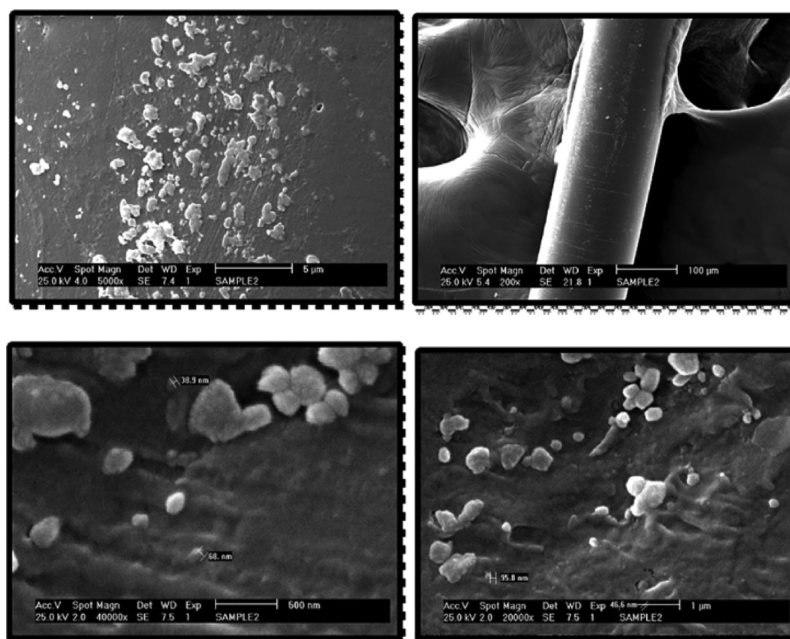


Figure 7. SEM of AgCl-NP synthesis on the PET fiber. 15 sequential dipping steps, ultrasound irradiation power 100 W, and pH = 9.

effective mixing in the layers of liquid. The impact of cavitation in non-homogenized systems is several hundred times more than that of homogenized systems.⁴⁹ Also, ultrasonic irradiation promotes the rapid migration of new nanoparticles to the surface of PET; therefore, in the presence of ultrasonic irradiation, there is no need of high temperature during the reaction, and the size of nanoparticles is smaller.^{31,50} Also, as shown in Figures 5–7, applying high-power ultrasonic irradiation causes the smaller size of nanoparticles.

2.2.2. pH Effect. The AgCl nanoparticles are synthesized in different pH: 5, 7, 9, and 11. According to the results (Figures 8–11), the average diameters of nanoparticles in pH 5, 7, 9, and 11 are 94.65, 70.77, 62.33, and 84.39 nm, respectively.

It can be concluded that the size of AgCl nanoparticles is reduced by increasing pH to 9, but in pH higher than 9, that is, pH 11, the AgCl nanoparticle size is increased, but the density of nanoparticles is decreased. The reason is that in higher pH, the opportunity of AgOH formation is more than that of the AgCl nanoparticle formation, and due to formation of AgOH sediments, the size of other nanoparticles will be increased.

2.2.3. Effects of Sequential Dipping Steps. In the synthesis of AgCl nanoparticles, to reach the optimum number of dipping steps in the reagent solutions, the reactions were carried out with three different numbers of dipping steps: 10, 15, and 20 times in pH = 9 and under the same condition. The results of SEM studies show that the average diameter of AgCl nanoparticles with a dipping step of 10, 15, and 20 times is

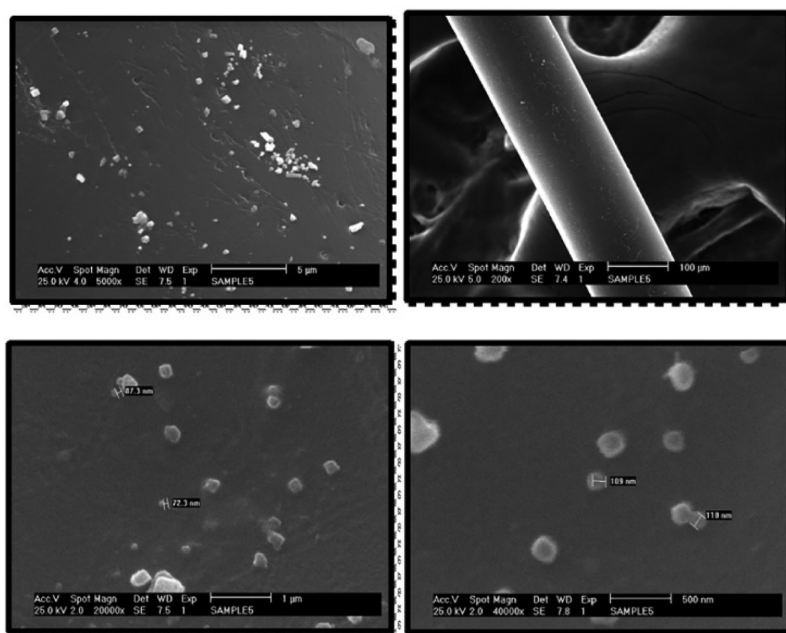


Figure 8. SEM of AgCl-NP synthesis on the PET fiber. 15 sequential dipping steps, ultrasound irradiation power 100 W, and pH = 5.

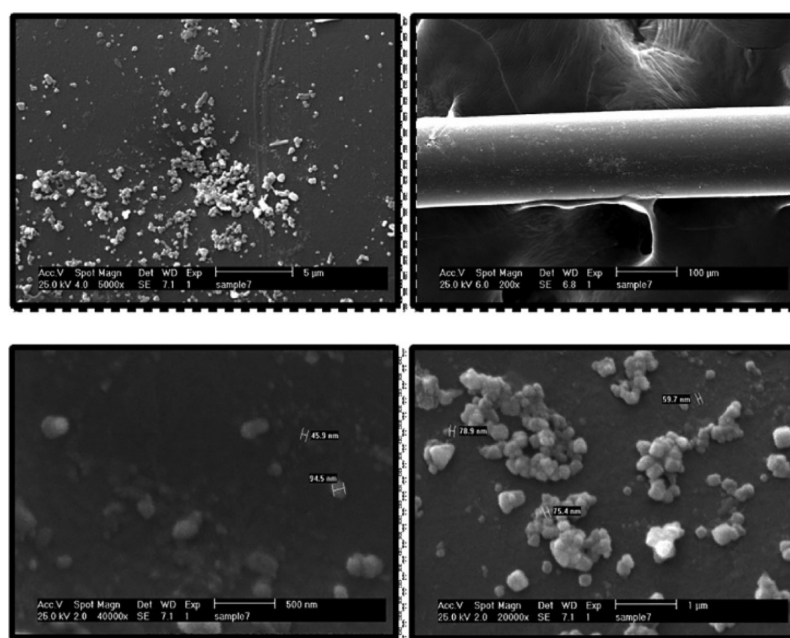


Figure 9. SEM of AgCl-NP synthesis on the PET fiber. 15 sequential dipping steps, ultrasound irradiation power 100 W, and pH = 7.

59.57, 62.33, and 62.75 nm, respectively (Figures 12–14). It can be concluded that by increasing the number of sequential dipping steps in AgNO_3 and KCl solutions, the time of reaction will be increased, and this leads to the increased growth, size, and number of AgCl nanoparticles.

The optimum number of dipping steps should lead to the lowest diameter (smallest size) and highest density of nanoparticles. By increasing the number of sequential dipping steps in the reagent solutions, the size of nanoparticles will increase, but as shown in the figures, in the samples that were sequentially dipped 15 times in the reagent solutions, the nanoparticle size is smaller than the size of those dipped 20 times in the reagent solutions.

In the synthesis of nanoparticles, not just the size but also the density of nanoparticles is important. In cycle 10 (dipping 10 times in the solutions), due to the lower number of nanoparticles, the density will be low too. However, in the higher cycles, the higher density of nanoparticles leads to higher distribution of size; therefore, cycle 15 was regarded as an optimum number of dipping steps. Summary results are shown in Table 1.

2.3. Bactericidal Tests. To investigate the antibacterial effect of AgCl nanoparticles on the surface of the PET polymer against two bacterial species, the modified PET polymer was added to the bacterial growth medium; after 18–24 h incubation, the results show no bacterial-growth zone due to the antibacterial properties of the modified PET polymer with

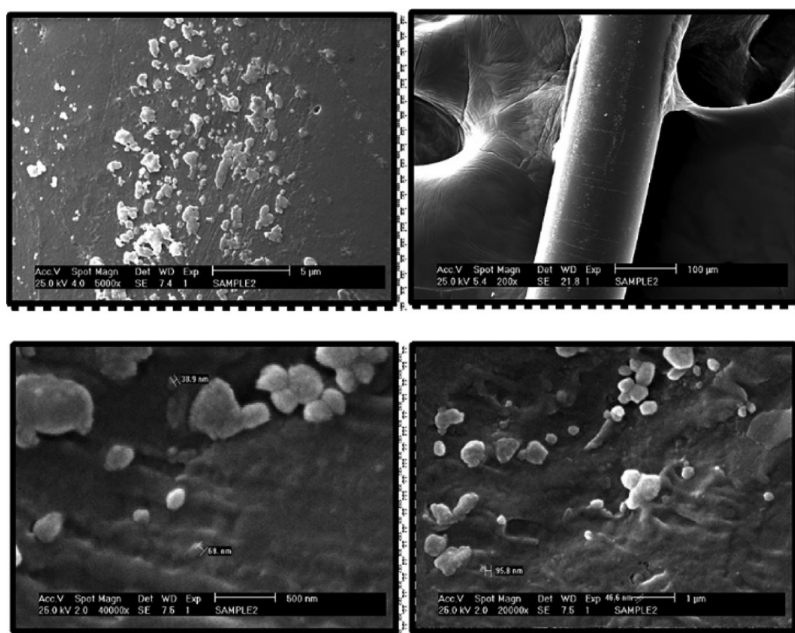


Figure 10. SEM of AgCl-NP synthesis on the PET fiber. 15 sequential dipping steps, ultrasound irradiation power 100 W, and pH = 9.

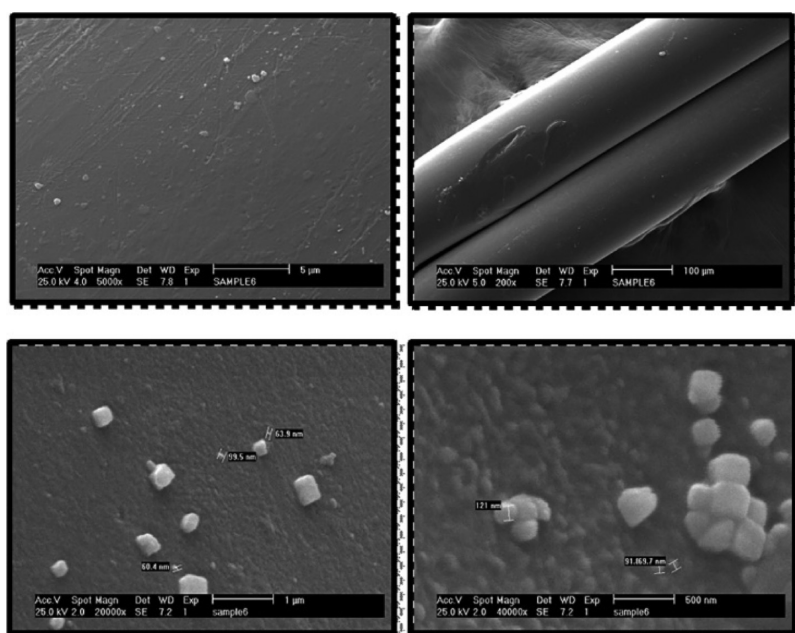


Figure 11. SEM of AgCl-NP synthesis on the PET fiber. 15 sequential dipping steps, ultrasound irradiation power 100 W, and pH = 11.

AgCl nanoparticles (Figure 15). AgCl nanoparticles synthesized on the PET surface showed the highest antibacterial activity against *Staphylococcus aureus* (ATCC 43300) and *Bacillus subtilis* (ATCC 6633).^{2,15,51}

3. CONCLUSIONS

PET was functionalized in two steps, and Fourier transform infrared spectroscopy (FT-IR) studies were performed to confirm the functionalization and the possible presence of carboxylic groups on the surface of the polymer. PET coated with AgCl nanoparticles was obtained by sequential dipping steps under ultrasonic irradiation. The effects of ultrasonic irradiation, sequential dipping steps, and pH on the growth of AgCl nanoparticles were studied. SEM images verify the

synthesis of AgCl nanoparticles on the surface of the PET polymer. Antibacterial activity of the modified surface was studied against two Gram-positive and Gram-negative bacterial species.

The results showed that in a power of 100 W, pH = 9, and cycle 15 (dipping 15 times in the solutions), AgCl nanoparticles can be synthesized with an average size of 62.33 nm and the maximum density on the surface of the functionalized polymer with the carboxylic group.

4. EXPERIMENTAL SECTION

4.1. Materials. PET fibers were supplied by Pouya Nakh Ilam Co. All the reagents and solvents were purchased from Merck chemical company and used without further purifica-

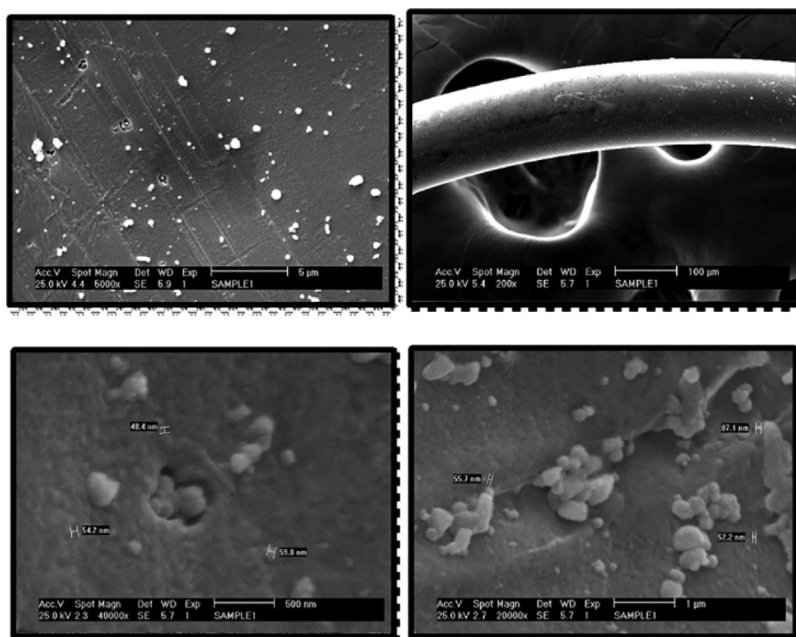


Figure 12. SEM of AgCl-NP synthesis on the PET fiber. 10 sequential dipping steps, ultrasound irradiation power 100 W, and pH = 9.

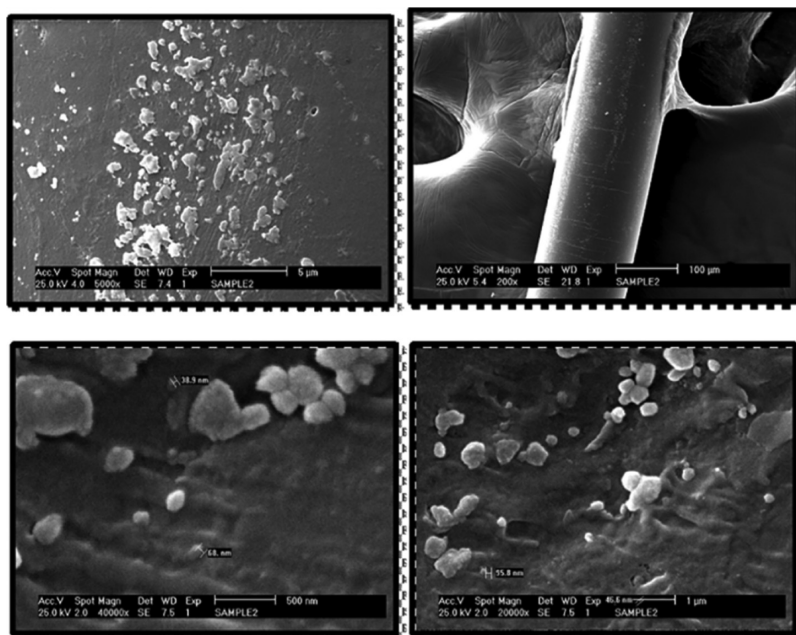


Figure 13. SEM of AgCl-NP synthesis on the PET fiber. 15 sequential dipping steps, ultrasound irradiation power 100 W, and pH = 9.

tion. To investigate the functionalization of PET, FT-IR (Vertex70) studies were used. SEM (Philip's Company, Netherlands) was applied to verify the synthesis of AgCl nanoparticles on the surface of PET. All the reactions were performed under different ultrasound irradiation powers (30 and 100 W) using Elmasonic P60H.

4.2. Methods. **4.2.1. Functionalization of PET.** 1 g of PET was rinsed with distilled water and ethanol and then dried for 3–4 h in an oven at 55 °C. PET functionalization was carried out in two steps: First, PET fibers were immersed in a solution of formaldehyde 18.5% and acetic acid 1 M for 4 h in room temperature. In the second step, PET was immersed in a solution of bromoacetic acid 1 M and NaOH 2 M for 18 h; then, it was rinsed with distilled water two times (for 15 min)

and dried in an oven for 48 h at 55 °C. The functionalized PET was characterized using FT-IR in order to verify the functionalization.^{8,52}

Figure 3 shows the synthesis of AgCl nanoparticles on the surface of PET; at the wavenumber lower than 800 cm^{-1} , peaks are formed, indicating the formation of nanoparticles on the surface of the PET and the creation of strong bonds between the metal and the surface of the polymer.²⁰

Based on Figure 4 of the XRD pattern mentioned below, the Miller indices at levels (111), (200), (220), and (311) correspond to the angles of 38.143, 25.465, 51.64, and 77.011°, respectively, which confirms the presence of silver nanoparticles on the surface of the modified PET polymer. The additional peaks are related to the impurities in the PET

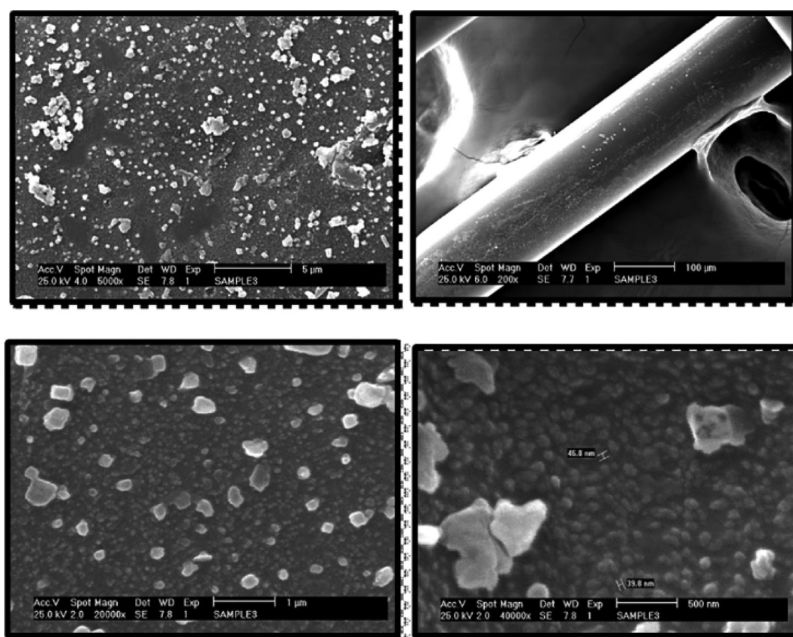


Figure 14. SEM of AgCl-NP synthesis on the PET fiber. 15 sequential dipping steps, ultrasound irradiation power 100 W, and pH = 20.

Table 1. Optimized Conditions of AgCl-NP Synthesis on Carboxylate PET

ultrasound effects ^a			
without ultrasound	high-power ultrasound	low-power ultrasound	
78.33 nm	62.33 nm	65.51 nm	
pH effect ^b			
pH = 5	pH = 7	pH = 9	pH = 11
94.65 nm	70.77 nm	62.33 nm	84.39 nm
effects of sequential dipping steps ^c			
10 steps	15 steps	20 steps	
59.57 nm	62.33 nm	62.75 nm	

^aOther conditions: pH = 9, sequential dipping steps = 15. ^bOther conditions: ultrasound power = 100 W, sequential dipping steps = 15. ^cOther conditions: pH = 9, ultrasound power = 100 W.

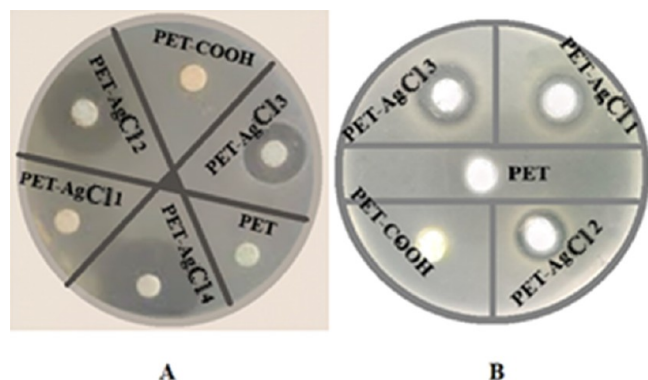


Figure 15. Pictures of the bactericidal test, (A) *Staphylococcus aureus* and (B) *Bacillus subtilis* by functionalized PET (PET-COOH), non-functionalized PET (PET), AgCl nanoparticles synthesized in pH 11 (PET-AgCl-NPs 1), AgCl nanoparticles synthesized in pH 9 and low power (PET-AgCl-NPs 2), and AgCl nanoparticles synthesized in pH 9 and high power (PET-AgCl-NPs 3).

polymer. Based on the studies performed and according to the crystalline plates expressed, it was found that silver is

crystallized in the structure of an FCC (cubic centers of total funds).

4.2.2. Coating of PET with AgCl Nanoparticles. The growth of AgCl nanoparticles on the surfaces of carboxylated PET fibers was reached by sequential dipping steps in an alternating bath of potassium chloride and silver nitrate under ultrasonic irradiation (frequency was constant 80 kHz for 20 min).

At first, the carboxylated PET polymer was placed in water, and the pH of this solution was adjusted to pH 9 with diluted potassium hydroxide. Then, sequential dipping of functionalized PET in AgNO₃ and KCl solutions was done. After bringing out the PET fibers from AgNO₃ solution, PET was washed in order to remove unattached ions. Dipping PET in KCl solution was followed by AgCl complex formation and initiation of AgCl nanoparticle formation. Repeating the sequential dipping steps in the alternating bath led to AgCl nanoparticle growth (Figure 16).

The duration time of the dipping step for each solution was 1 min followed by a 1 min washing step.⁴⁸ At the end of the modification process, the samples were dried for 24 h in an oven at 55 °C. In order to study the effect of ultrasonic irradiation on the synthesis and size of nanoparticles, all the experiments were performed in a power of 30 and 100 W. To investigate the influence of pH on AgCl nanoparticle synthesis, solutions were prepared in a pH range of 5–11. All steps of AgCl nanoparticle formation were carried out on the surface of PET in different numbers of dipping steps to reach an optimum number of dipping cycles.⁵³

4.2.3. Bactericidal Tests. After preparing nutrient Muller-Hinton agar medium in the plates, 4 mm diameter wells were made in the medium using a Pasteur pipette (well diffusion method). Next, certain amounts of modified PET coatings with different amounts of AgCl nanoparticles, functionalized and non-functionalized PET, were put in the wells of plates (weight-wise). In the next step, two different bacterial species were added to the wells separately followed by incubation for 18–24 h to study the inhibition growth zone as an indicator of

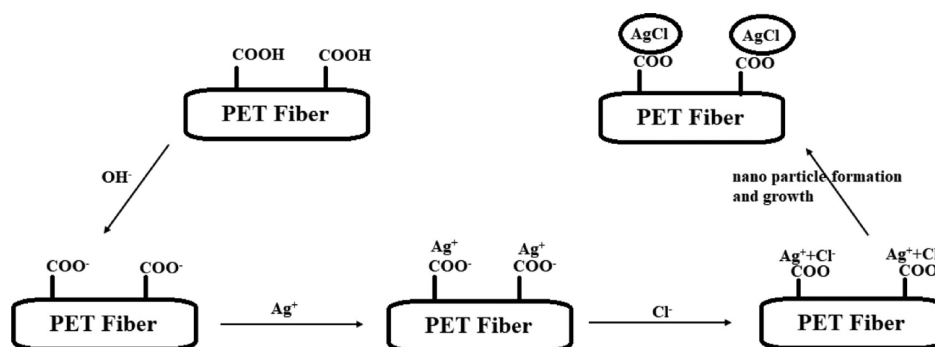


Figure 16. Scheme of the AgCl-NP synthesis mechanism on the PET fiber.

antibacterial activity of modified PET with AgCl nanoparticles against these two different bacterial species:

- *Staphylococcus aureus* (ATCC 43300) and
- *B. subtilis* (ATCC 6633).

AUTHOR INFORMATION

Corresponding Authors

Hossein Peyman – Department of Chemistry, Ilam Branch, Islamic Azad University, Ilam, Iran;
Phone: +988432228074; Email: peymanhossein@gmail.com

Shohreh Azizi – UNESCO-UNISA Africa Chair in Nanosciences and Nanotechnology, College of Graduate Studies, University of South Africa, Pretoria 0002, South Africa; Nanosciences African Network (NANOAFNET), iThemba LABS-National Research Foundation, Somerset West, Western Cape 7131, South Africa; orcid.org/0000-0003-0419-9953; Email: shohrehazizi1379@gmail.com, azizis@unisa.ac.za

Authors

Mitra Alidadykhah – Department of Chemistry, Ilam Branch, Islamic Azad University, Ilam, Iran

Hamideh Roshanfekr – Department of Chemistry, Ilam Branch, Islamic Azad University, Ilam, Iran

Malik Maaza – UNESCO-UNISA Africa Chair in Nanosciences and Nanotechnology, College of Graduate Studies, University of South Africa, Pretoria 0002, South Africa; Nanosciences African Network (NANOAFNET), iThemba LABS-National Research Foundation, Somerset West, Western Cape 7131, South Africa

Complete contact information is available at:

<https://pubs.acs.org/10.1021/acsomega.1c07082>

Notes

The authors declare no competing financial interest.

ACKNOWLEDGMENTS

Support of this investigation by the Ilam branch of Islamic Azad University is gratefully acknowledged.

REFERENCES

- (1) Seyedalizadeh, M.; Abdolmaleki, F. The Effect of Microwave on Migration of Styrene Monomer Polystyrene Food Packaging and Compared to other Thermal Processes. *J. Food Biosci. Technol.* **2019**, *9*, 69–76.
- (2) Wang, Z.; Bates, F. S.; Macosko, C. W.; Wang, K.; Haberkamp, W. C.; Holm, C. E. Tuning surface properties of melt blown polyester

fibers by hydrolysis and solution grafting. Google Patents US 10,227,725B2, 2019.

(3) Nerantzaki, M.; Prokopiou, L.; Bikiaris, D. N.; Patsiaoura, D.; Chrissafis, K.; Klonos, P.; Kyritsis, A.; Pissis, P. In situ prepared poly (DL-lactic acid)/silica nanocomposites: Study of molecular composition, thermal stability, glass transition and molecular dynamics. *Thermochim. Acta* **2018**, *669*, 16–29.

(4) Babaei, A.; Aminikhah, M.; Taheri, A. R. A multi-walled carbon nano-tube and nickel hydroxide nano-particle composite-modified glassy carbon electrode as a new sensor for the sensitive simultaneous determination of ascorbic acid, dopamine and uric acid. *Sens. Lett.* **2013**, *11*, 413–422.

(5) Haulon, S.; Devos, P.; Willoteaux, S.; Mounier-Vehier, C.; Sokoloff, A.; Halna, P.; Beregi, J. P.; Koussa, M. Risk factors of early and late complications in patients undergoing endovascular aneurysm repair. *Eur. J. Vasc. Endovasc. Surg.* **2003**, *25*, 118–124.

(6) Grumezescu, A. M.; Stoica, A. E.; Dima-Bălcescu, M.-Ș.; Chircov, C.; Gharbia, S.; Baltă, C.; Roșu, M.; Herman, H.; Holban, A. M.; Fica, A.; Vasile, B. S.; Andronescu, E.; Chifiriuc, M. C.; Hermenean, A. Dima-Bălcescu M-Ș, Chircov C, Gharbia S, Baltă C, Roșu M, Herman H, Holban AM, Fica A. Electrospun polyethylene terephthalate nanofibers loaded with silver nanoparticles: novel approach in anti-infective therapy. *J. Clin. Med.* **2019**, *8*, 1039.

(7) Ramachandran, B.; Chakraborty, S.; Dixit, M.; Muthuvijayan, V. A comparative study of polyethylene terephthalate surface carboxylation techniques: Characterization, in vitro haemocompatibility and endothelialization. *React. Funct. Polym.* **2018**, *122*, 22–32.

(8) Muthuvijayan, V.; Gu, J.; Lewis, R. S. Analysis of functionalized polyethylene terephthalate with immobilized NTPDase and cysteine. *Acta Biomater.* **2009**, *5*, 3382–3393.

(9) Mohammed, R. A.; Saleh, K. A. Conducting Poly [N-(4-Methoxy Phenyl) Maleamic Acid]/Metals Oxides Nanocomposites for Corrosion Protection and Bioactivity Applications. *Chem. Methodol.* **2022**, *6*, 74–82.

(10) Wyssusek, K.; Keys, M.; Laycock, B.; Avudainayagam, A.; Pun, K.; Hansraj, S.; van Zundert, A. The volume of recyclable polyethylene terephthalate plastic in operating rooms—A one-month prospective audit. *Am. J. Surg.* **2020**, *220*, 853–855.

(11) Zieren, J.; Neuss, H.; Paul, M.; Müller, J. Introduction of polyethylene terephthalate mesh (KoSa hochfest®) for abdominal hernia repair: An animal experimental study. *Bio-Med. Mater. Eng.* **2004**, *14*, 127–132.

(12) Heydarzadeh, S.; Roshanfekr, H.; Peyman, H.; Kashanian, S. Modeling of ultrasensitive DNA hybridization detection based on gold nanoparticles/carbon-nanotubes/chitosan-modified electrodes. *Colloids Surf., A* **2020**, *587*, 124219.

(13) Gangadharan, S.; Sujith, A.; Anbazhagan, V. Preparation and Characterization of Hybrid Biocomposite Based on Woven Palm-Cotton Fibers and Used Expanded Polystyrene Beads. *Chem. Methodol.* **2021**, *5*, 555–564.

(14) Gappa-Fahlenkamp, H.; Lewis, R. S. Improved hemocompatibility of poly (ethylene terephthalate) modified with various thiol-containing groups. *Biomaterials* **2005**, *26*, 3479–3485.

- (15) Li, J.; Liu, X.; Lu, J.; Wang, Y.; Li, G.; Zhao, F. Anti-bacterial properties of ultrafiltration membrane modified by graphene oxide with nano-silver particles. *J. Colloid Interface Sci.* **2016**, *484*, 107–115.
- (16) Farmani, M. R.; Peyman, H.; Roshanfekr, H. Blue luminescent graphene quantum dot conjugated cysteamine functionalized-gold nanoparticles (GQD-AuNPs) for sensing hazardous dye Erythrosine B. *Spectrochim. Acta, Part A* **2020**, *229*, 117960.
- (17) Yang, Z.; Belu, A. M.; Liebmann-Vinson, A.; Sugg, H.; Chilkoti, A. Molecular imaging of a micropatterned biological ligand on an activated polymer surface. *Langmuir* **2000**, *16*, 7482–7492.
- (18) Reverchon, E.; Adami, R. Nanomaterials and supercritical fluids. *J. Supercrit. Fluids* **2006**, *37*, 1–22.
- (19) Basnet, P.; Chatterjee, S. Structure-directing property and growth mechanism induced by capping agents in nanostructured ZnO during hydrothermal synthesis—A systematic review. *Nano-Struct. Nano-Objects* **2020**, *22*, 100426.
- (20) Rostamnia, S.; Doustkhah, E.; Estakhri, S.; Karimi, Z. Layer by layer growth of silver chloride nanoparticle within the pore channels of SBA-15/SO₃H mesoporous silica (AgClNP/SBA-15/SO₃K): Synthesis, characterization and antibacterial properties. *Phys. E* **2016**, *76*, 146–150.
- (21) Ahadi, A.; Alamgholiloo, H.; Rostamnia, S.; Liu, X.; Shokouhimehr, M.; Alonso, D. A.; Luque, R. Layer-Wise Titania Growth Within Dimeric Organic Functional Group Viologen Periodic Mesoporous Organosilica as Efficient Photocatalyst for Oxidative Formic Acid Decomposition. *ChemCatChem* **2019**, *11*, 4803–4809.
- (22) Abbasi, A. R.; Morsali, A. Syntheses and characterization of AgI nano-structures by ultrasonic method: different morphologies under different conditions. *Ultrason. Sonochem.* **2010**, *17*, 572–578.
- (23) Tomšič, B.; Simončič, B.; Orel, B.; Žerjav, M.; Schroers, H.; Simončič, A.; Samardžija, Z. Antimicrobial activity of AgCl embedded in a silica matrix on cotton fabric. *Carbohydr. Polym.* **2009**, *75*, 618–626.
- (24) Bai, J.; Li, Y.; Li, M.; Wang, S.; Zhang, C.; Yang, Q. Electrospinning method for the preparation of silver chloride nanoparticles in PVP nanofiber. *Appl. Surf. Sci.* **2008**, *254*, 4520–4523.
- (25) Tiwari, J.; Rao, C. Template synthesized high conducting silver chloride nanoplates. *Solid State Ionics* **2008**, *179*, 299–304.
- (26) Husein, M.; Rodil, E.; Vera, J. H. Formation of silver bromide precipitate of nanoparticles in a single microemulsion utilizing the surfactant counterion. *J. Colloid Interface Sci.* **2004**, *273*, 426–434.
- (27) Husein, M. M.; Rodil, E.; Vera, J. H. A novel method for the preparation of silver chloride nanoparticles starting from their solid powder using microemulsions. *J. Colloid Interface Sci.* **2005**, *288*, 457–467.
- (28) Rahimi, F.; Roshanfekr, H.; Peyman, H. Ultra-sensitive electrochemical aptasensor for label-free detection of Aflatoxin B1 in wheat flour sample using factorial design experiments. *Food Chem.* **2021**, *343*, 128436.
- (29) Spirin, M. G.; Brichkin, S. B.; Razumov, V. F. Growth kinetics for AgI nanoparticles in AOT reverse micelles: Effect of molecular length of hydrocarbon solvents. *J. Colloid Interface Sci.* **2008**, *326*, 117–120.
- (30) Hu, W.; Chen, S.; Li, X.; Shi, S.; Shen, W.; Zhang, X.; Wang, H. In situ synthesis of silver chloride nanoparticles into bacterial cellulose membranes. *Mater. Sci. Eng., C* **2009**, *29*, 1216–1219.
- (31) Zhao, L.; Wang, Y.; Chen, Z.; Zou, Y. Preparation, characterization, and optical properties of host-guest nanocomposite material SBA-15/AgI. *Phys. B* **2008**, *403*, 1775–1780.
- (32) Ghasemi, J.; Peyman, H.; Niazi, A. Spectrophotometric Determination of Acidity Constants of 4-(2-Pyridylazo) Resorcinol in Various Micellar Media Solutions. *J. Chin. Chem. Soc.* **2007**, *54*, 1093–1097.
- (33) Valdižić, I. L.; Jakanović, V.; Uskoković, D. P.; Nedeljković, J. M. Influence of solvent on the structural and morphological properties of AgI particles prepared using ultrasonic spray pyrolysis. *Mater. Chem. Phys.* **2008**, *107*, 28–32.
- (34) Abbasi, A. R.; Morsali, A. Formation of silver iodide nanoparticles on silk fiber by means of ultrasonic irradiation. *Ultrason. Sonochem.* **2010**, *17*, 704–710.
- (35) Sharipov, G. L.; Gareev, B. M.; Abdrakhmanov, A. M. Spectroscopic measurement of electronic temperature in the bubbles during single- and multibubble sonoluminescence of metal carbonyl solutions and nanodispersed suspensions. *Ultrason. Sonochem.* **2019**, *51*, 178–181.
- (36) Gedanken, A. Using sonochemistry for the fabrication of nanomaterials. *Ultrason. Sonochem.* **2004**, *11*, 47–55.
- (37) Khanjani, S.; Morsali, A. A new nano-particles LaIII compound as a precursor for preparation of La₂O₂(SO₄) nano-particles. *J. Mol. Struct.* **2009**, *935*, 27–31.
- (38) Alidadykhoh, M.; Pyman, H.; Roshanfekr, H. Application of a New Polymer AgCl Nanoparticles Coated Polyethylene Terephthalat [PET] as Adsorbent for Removal and Electrochemical Determination of Methylene Blue Dye. *Chem. Methodol.* **2021**, *5*, 96–106.
- (39) Unnarkat, A. P.; Sridhar, T.; Wang, H.; Mahajani, S. M.; Suresh, A. K. Study of cobalt molybdenum oxide supported on mesoporous silica for liquid phase cyclohexane oxidation. *Catal. Today* **2018**, *310*, 116–129.
- (40) Alavi, M. A.; Morsali, A. Syntheses and characterization of Sr(OH)₂ and SrCO₃ nanostructures by ultrasonic method. *Ultrason. Sonochem.* **2010**, *17*, 132–138.
- (41) Fattahi, M.; Ezzatzadeh, E.; Jalilian, R.; Taheri, A. Micro solid phase extraction of cadmium and lead on a new ion-imprinted hierarchical mesoporous polymer via dual-template method in river water and fish muscles: Optimization by experimental design. *J. Hazard. Mater.* **2021**, *403*, 123716.
- (42) Mohammadi, M.; Morsali, A. Different thallium(III) oxide nano-structures from direct thermal decomposition of two thallium(I) coordination polymers. *Mater. Lett.* **2009**, *63*, 2349–2351.
- (43) Soltanzadeh, N.; Morsali, A. Sonochemical synthesis of a new nano-structures bismuth(III) supramolecular compound: New precursor for the preparation of bismuth(III) oxide nano-rods and bismuth(III) iodide nano-wires. *Ultrason. Sonochem.* **2010**, *17*, 139–144.
- (44) Potiyaraj, P.; Kumlangdudsana, P.; Dubas, S. T. Synthesis of silver chloride nanocrystal on silk fibers. *Mater. Lett.* **2007**, *61*, 2464–2466.
- (45) Lalabadi, M. A.; Peyman, H.; Roshanfekr, H.; Azizi, S.; Maaza, M. Polyethersulfone nanofiltration membrane embedded by magnetically modified MOF (MOF@ Fe₃O₄): fabrication, characterization and performance in dye removal from water using factorial design experiments. *Polym. Bull.* **2022**, *1–21*.
- (46) Kim, K.-H.; Kim, K.-B. Ultrasound assisted synthesis of nano-sized lithium cobalt oxide. *Ultrason. Sonochem.* **2008**, *15*, 1019–1025.
- (47) Ullah, H.; Yamani, Z. H.; Qurashi, A.; Iqbal, J.; Safeen, K. Study of the optical and gas sensing properties of In₂O₃ nanoparticles synthesized by rapid sonochemical method. *J. Mater. Sci.: Mater. Electron.* **2020**, *31*, 17474–17481.
- (48) Abbasi, A. R.; Bohloulzadeh, M.; Morsali, A. Preparation of AgCl nanoparticles@ ancient textile with antibacterial activity under ultrasound irradiation. *J. Inorg. Organomet. Polym. Mater.* **2011**, *21*, 504–510.
- (49) Perelshtein, I.; Applerot, G.; Perkas, N.; Wehrschuetz-Sigl, E.; Hasmann, A.; Guebitz, G.; Gedanken, A. CuO-cotton nanocomposite: Formation, morphology, and antibacterial activity. *Surf. Coat. Technol.* **2009**, *204*, 54–57.
- (50) Perkas, N.; Amirian, G.; Dubinsky, S.; Gazit, S.; Gedanken, A. Ultrasound-assisted coating of nylon 6,6 with silver nanoparticles and its antibacterial activity. *J. Appl. Polym. Sci.* **2007**, *104*, 1423–1430.
- (51) Al-Kaysi, R. O.; Müller, A. M.; Ahn, T.-S.; Lee, S.; Bardeen, C. J. Effects of sonication on the size and crystallinity of stable zwitterionic organic nanoparticles formed by reprecipitation in water. *Langmuir* **2005**, *21*, 7990–7994.
- (52) Alamgholiloo, H.; Rostamnia, S.; Hassankhani, A.; Liu, X.; Eftekhari, A.; Hasanzadeh, A.; Zhang, K.; Karimi-Maleh, H.; Khaksar, S.; Varma, R. S.; Shokouhimehr, M. Formation and stabilization of

colloidal ultra-small palladium nanoparticles on diamine-modified Cr-MIL-101: Synergic boost to hydrogen production from formic acid. *J. Colloid Interface Sci.* **2020**, *567*, 126–135.

(53) Liu, Y.; Chen, J.-R.; Yang, Y.; Wu, F. Improved blood compatibility of poly (ethylene terephthalate) films modified with L-arginine. *J. Biomater. Sci., Polym. Ed.* **2008**, *19*, 497–507.